

# An Off-Axis Zone-Plate Monochromator for High-Power Undulator Radiation

M. R. Howells\*, P. Charalambous%, H. He\*, S. Marcesini\*, J. C. H. Spence\*#

\*Advanced Light Source, Lawrence Berkeley National Laboratory

#Dept. of Physics, Arizona State University

%King's College London

## ABSTRACT

We report the design and construction of an off-axis zone-plate monochromator for diffraction-imaging experiments at beam line 9.0.1 at the Advanced Light Source (ALS) synchrotron-radiation facility at Berkeley USA. The device is based on an off-axis zone plate which can be conveniently inserted into or retracted from the beam. We discuss design issues such as the efficiency and spectral purity of the system and the technique for designing heat-tolerant windows for soft x-ray undulator beams. The monochromator functions successfully and good-quality diffractions patterns are being made with the beam it delivers.

**Keywords:** zone plate, monochromator, undulator, diffraction imaging

## 1. INTRODUCTION

Zone plate monochromators have been used in synchrotron radiation beam lines for some time, mostly by the Gottingen group as condensers for zone-plate x-ray microscopes<sup>6</sup> and this has recently included an undulator beam line at BESSY<sup>5</sup> Undulator beams introduce additional difficulties because of the increased x-ray beam power. Our requirement for a zone plate monochromator arose because we needed to share a pink beam (a once-reflected but unmonochromatized undulator beam) between two users one of which needed the pink beam while the other (ourselves) needed a beam with narrower bandwidth (around  $10^{-3}$ ) for diffraction-imaging experiments. Since our application was not a zone-plate microscope, the requirement was not for a hollow-cone beam but rather for uniform illumination of a sample several microns in width. Thus a scheme using an off-axis segment of a zone plate was suitable and also satisfied the need to be easily inserted and removed without compromising the delivery of the pink beam. We describe the design of the monochromator and our operational experiences with it in what follows.

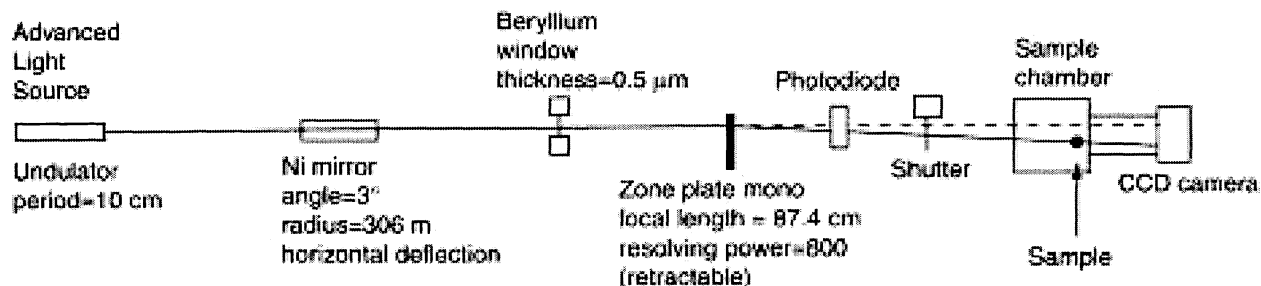


Fig. 1. Beam line overview from the side

## 2. BEAM LINE DESIGN

An overview of the beam line is shown in Figure 1. (above). The diffraction experiments are to be done at 588 eV in undulator 3rd harmonic. The Be window is 0.8 mm diameter which defines the beam size and thus the zone-plate size. A resolving power of 800-1000 is required (compared to about 100 for the pink beam). We will discuss the spectral output of the source and the beam line as a whole in a later section.

## 3. ZONE PLATE MONOCHROMATOR: OPTICAL DESIGN

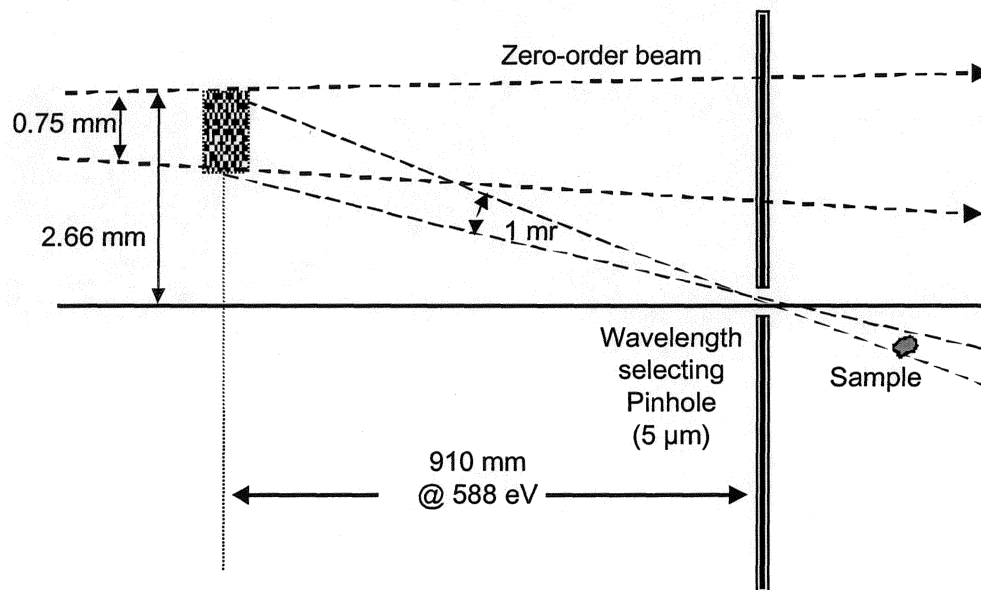


Figure 2. General monochromator layout

The zone plate optical parameters are as follows:

Zone plate nominal operating energy = 600 eV

Focal length = 0.874 m

Diameter (of complete mathematical zone plate) = 5.31 mm

Outer zone width = 0.34  $\mu\text{m}$

Object distance = 23.3 m

Image distance = 0.91 m

Vertical demagnification = 25.7

X-ray vertical spot sizes:

Geometrical image size = 2.3  $\mu\text{m}$

Diffraction size = 2.3  $\mu\text{m}$

Combined size = 3.3  $\mu\text{m}$

Resolving power (based on combined spot size) = 802

Number of zone plate periods in segment = 1000

#### 4. ZONE-PLATE DESIGN AND MANUFACTURING

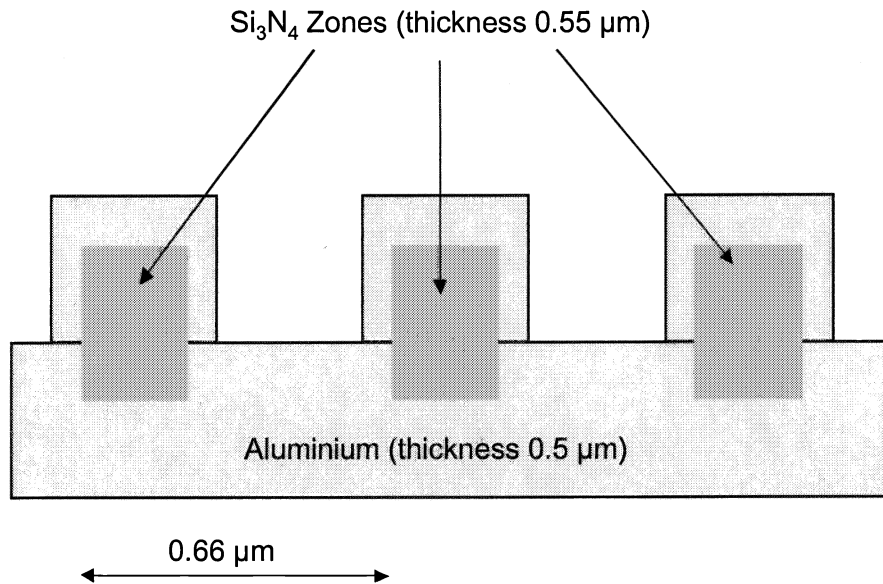


Figure 3. Mechanical layout of the zone plate to be manufactured by the following steps (1) coat one side of a 0.55 μm thick silicon nitride window with aluminum, (2) e-beam write and etch the zone-plate pattern into the silicon nitride material and (3) coat the other side of the window with aluminum such that the total vertical thickness of aluminum is 0.5 μm.

The zone plate was made as shown in Figure 3 so that the rings were cut in silicon nitride which was therefore the principle optical material providing diffraction to a focus. The purpose of the aluminum on both sides was to provide mechanical stability and the best possible heat removal pathway consistent with the required x-ray transparency.

#### 5. ZONE PLATE EFFICIENCY

The thickness of the silicon nitride rings was chosen as the closest available window thickness to the  $\pi$  phase-shift thickness for this material at the nominal operating energy of 600 eV. The zone plate efficiency  $E_n$  in  $n$ th order can then be calculated according to the prescription of Kirz<sup>4</sup>

$$E_n = \frac{1}{n^2 \pi^2} (1 + r^2 - 2r \cos \phi) \quad \text{with } r = e^{-k\beta}, \quad \phi = kz\delta$$

where  $z$  is the thickness,  $k$  is  $2\pi$  divided by the x-ray wavelength and  $\delta$  and  $\beta$  are the real and imaginary parts respectively of the unit decrement of the complex refractive index. The efficiencies in +1 order of several candidate materials are plotted in Figure 4. The mark-to-space ratio is taken to have its optimum value of 0.5

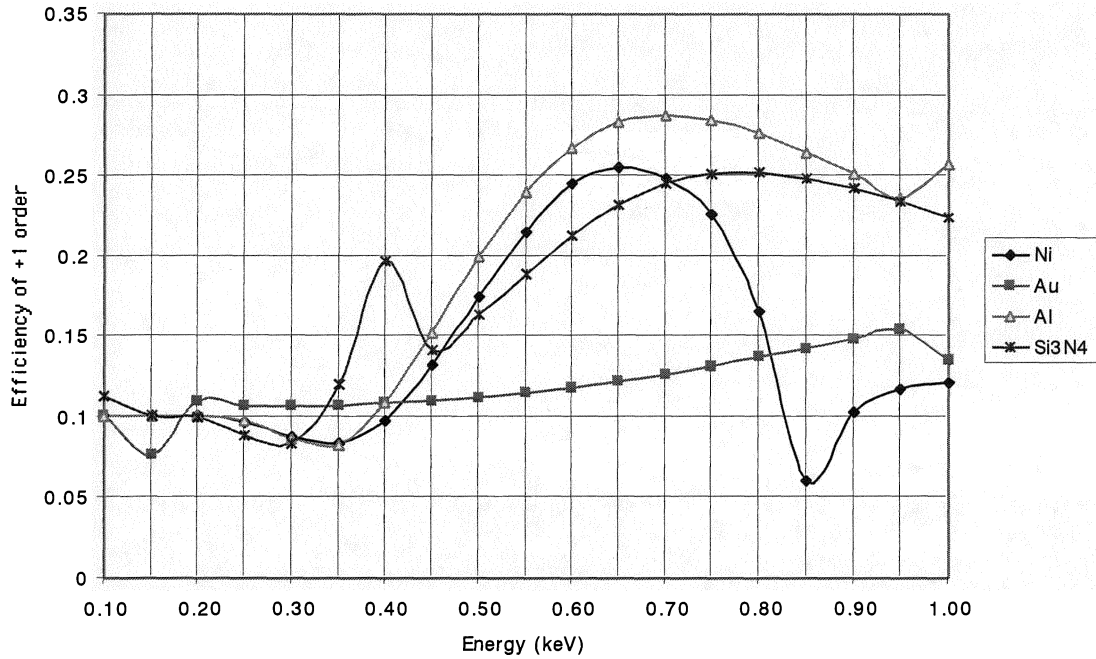


Figure 4. Calculated efficiencies of Ni, Au, Al and silicon nitride as a function of photon energy for a thin zone plate

The spectral output of the beam line is determined by the source and optical components, i. e. the nickel mirror, beryllium window and the zone plate. The efficiencies of the components are shown in Figure 5.

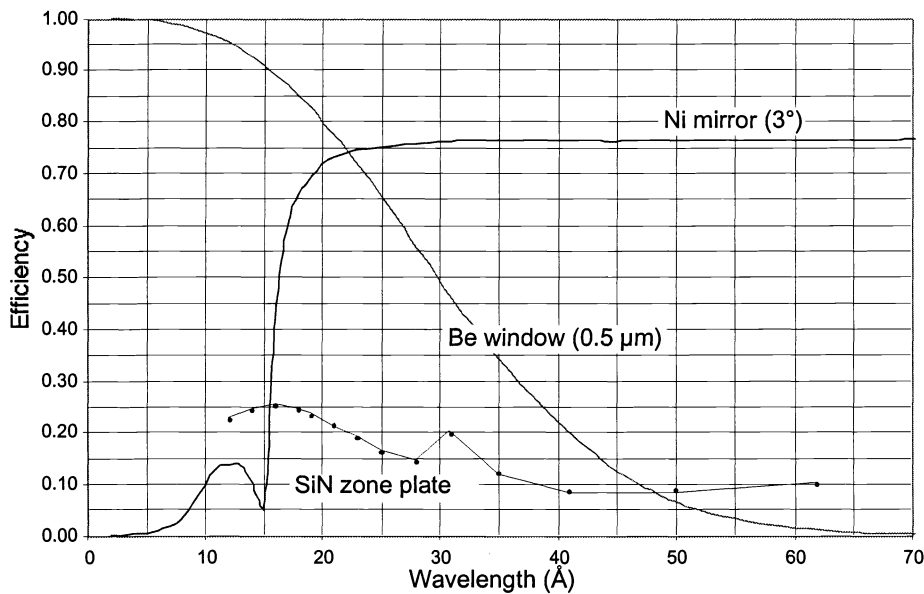


Fig. 5. X-ray efficiencies of the mirror (3° nickel), window (0.5 μm beryllium) and zone plate (0.55 μm silicon nitride)

It is evident that a region of good efficiency exists around 20-25 Å which would be too narrow for most spectroscopy applications but is quite good for imaging experiments.

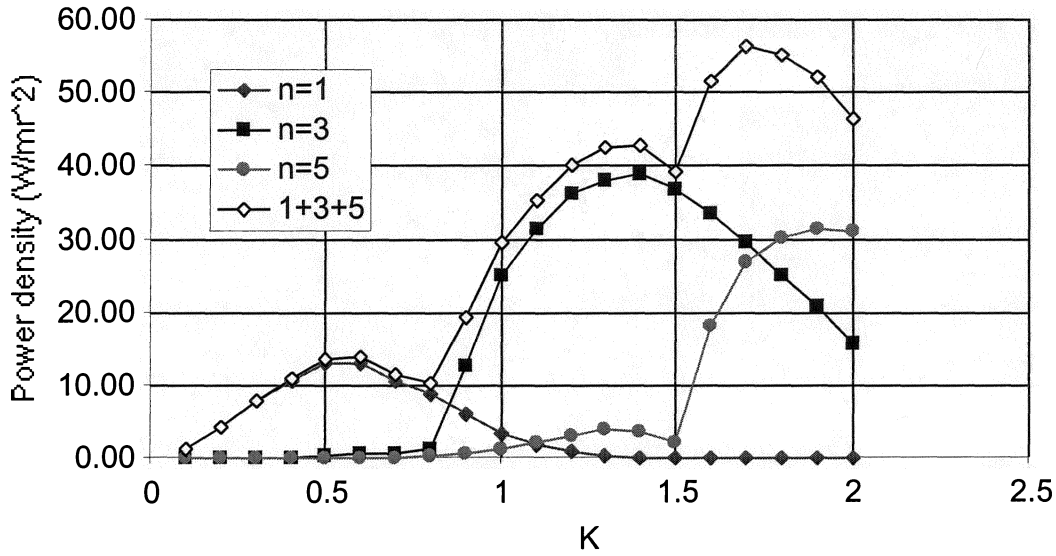


Fig. 6. Output of the whole beam line including the mirror and window but not the zone plate as a function of  $K$

The 10-cm-period undulator is designed principally for low-energy spectroscopy down to near-UV photon energies so one does not expect good soft-x-ray performance in the first harmonic. However the third harmonic provides 20-25 Å radiation in the region roughly from  $K$  equals 1 to 1.5. Figure 6 shows that this corresponds to a region of rather good spectral purity. This arises because the first (low energy) harmonic is largely killed by the beryllium window and the 5<sup>th</sup> (high energy) harmonic is killed by the mirror.

## 6. GENERAL PROBLEM OF HEATING OF A UNIFORMLY ILLUMINATED RECTANGULAR X-RAY WINDOW

The Fourier equation for the two-dimensional heat-flow problem in Cartesian coordinates  $x, y$  is as follows.

$$\frac{\partial^2 T}{\partial x^2} + \frac{\partial^2 T}{\partial y^2} = -\frac{Q}{kt}$$

where  $T$  is the temperature,  $k$  the conductivity,  $t$  the window thickness and  $Q$  the power absorbed per unit area<sup>2</sup>. For our problem,  $Q$  is a known constant but the above equation has still to be taken as a Poisson (not a Laplace) equation. It can be solved by standard methods such as Navier's<sup>7</sup> or Green's<sup>1</sup> and assuming a thin window of size  $a \times b$  surrounded by a thick frame which is taken (without loss of generality) to be at  $T=0$ , the solution is

$$T(x,y) = \frac{16Q}{\pi^4 kt} \sum_{\substack{m=1 \\ m,n}}^{\infty} \sum_{\substack{n=1 \\ odd}}^{\infty} \frac{1}{mn} \frac{\sin \frac{m\pi x}{a} \sin \frac{n\pi y}{b}}{\frac{m^2}{a^2} + \frac{n^2}{b^2}}$$

For a square window the double sum becomes a universal function  $S(x/a, y/a)$  with a maximum  $S(1/2, 1/2) = 0.448$  at the center. We thus get a simple and useful expression for the center temperature relative to the frame as zero

$$T_{\max} = 7.17 \frac{Qa^2}{\pi^4 kt}$$

The function  $S(x/a, y/a)$  is plotted for  $y = a/2$  in Figure 7.

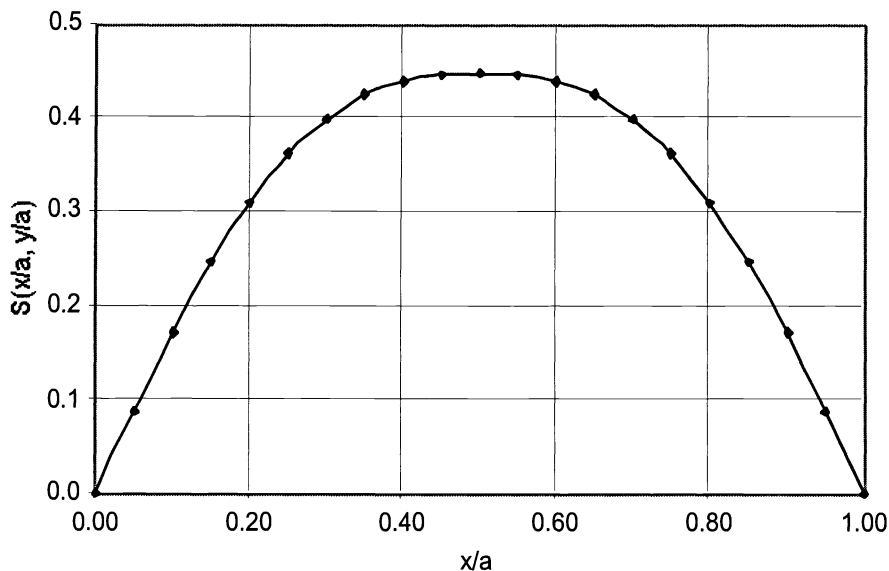


Fig. 7. Universal function describing the temperature distribution over an x-ray-heated square window. The plot is taken along the line  $y=a/2$

## 7. THE POWER ABSORPTION ISSUE IN THE WINDOWS IN OUR BEAM LINE

The above analysis was applied to both the beryllium window and the zone plate on our beam line. The essential reasons for our success in designing windows that could survive normal-incidence illumination by an ALS undulator were the power filtering of the mirror and the smallness and high transparency of the windows. The beryllium window (0.8 mm diameter, 0.5  $\mu\text{m}$  thick) was epoxied to a copper ring by the manufacturer<sup>3</sup> and the ring was clamped to a cooled copper block across a tapered 0.8 mm hole in the block. The beam was several mm wide (depending on  $K$ ) at this point so the majority of the beam power was deposited in the cooled copper block.

The zone plate was built from a 0.75 mm square silicon nitride window by the method described earlier. The silicon frame of the window was 0.5 mm thick, i. e. much thicker than the zone plate, and the frame was epoxied to an aluminum block mounted on a large x-y positioning device<sup>8</sup>. No water cooling was applied to the zone-plate system.

The arriving power density at the zone plate due to the first three harmonics is:

$$n=1: 0.006 \text{ W/mm}^2$$

$$n=3: 0.319 \text{ W/mm}^2$$

$n=5$ :  $0.043 \text{ W/mm}^2$

while the overall absorbed power is  $0.236 \text{ W/mm}^2$ . This is calculated for a  $0.5 \mu\text{m}$  thick aluminum window with  $0.55 \mu\text{m}$  of silicon nitride spread over 50% of its area. The calculated center temperature by the above method was  $80^\circ\text{C}$ .

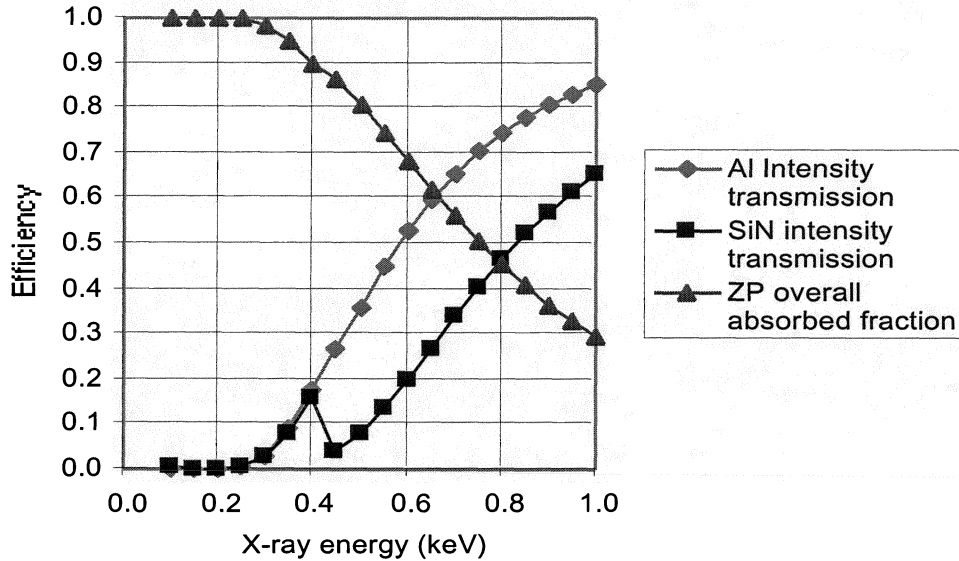


Fig. 8. X-ray absorption by the aluminum and silicon nitride parts of the zone plate. Note that around our operating energy of 0.6 keV most of the power is absorbed in the silicon nitride

Figure 8 shows the power absorption in the aluminum and silicon nitride parts of the zone plate. It is noteworthy that the center temperature calculated above is proportional to  $Q/t$ . This shows that for a simple x-ray window the temperature reached is roughly independent of the thickness because  $Q$  will increase linearly with  $t$ . However this is not the case for a composite window as we have here where the majority of the power is absorbed in a second material mounted on the window. To get the best heat tolerance, we thus increase the aluminum thickness as much as possible consistent with transparency requirements.

## 8. ZONE PLATE PERFORMANCE AS A MONOCHROMATOR

Figure 9 shows the photocurrent in a detector placed behind a  $25 \mu\text{m}$  slit placed 8 cm upstream of the zone-plate focus. The slit is mechanically scanned vertically across the illuminated field in steps of 10, 20 and  $50 \mu\text{m}$  as shown in the legend. The slightly-out-of-focus spots delivered by the zone plate at the slit can be viewed on phosphor on the upstream side of the slit via a 45-degree mirror fixed to the slit plate. The plots in Figure 9 show various orders of the zone plate combined with various harmonics of the undulator, the latter being set for 588 eV in the third harmonic. The principal peak, other than zero order is the desired one which is used for experiments. The contributions to the width of this peak are as follows.

Diffraction:  $2.3 \mu\text{m}$

Geometrical image:  $2.3 \mu\text{m}$

Source bandwidth:  $20 \mu\text{m}$

Slit size:  $25 \mu\text{m}$

Defocus:  $90 \mu\text{m}$

From these the calculated width is 96  $\mu\text{m}$  which agrees reasonably well with the measured width of 110  $\mu\text{m}$ .

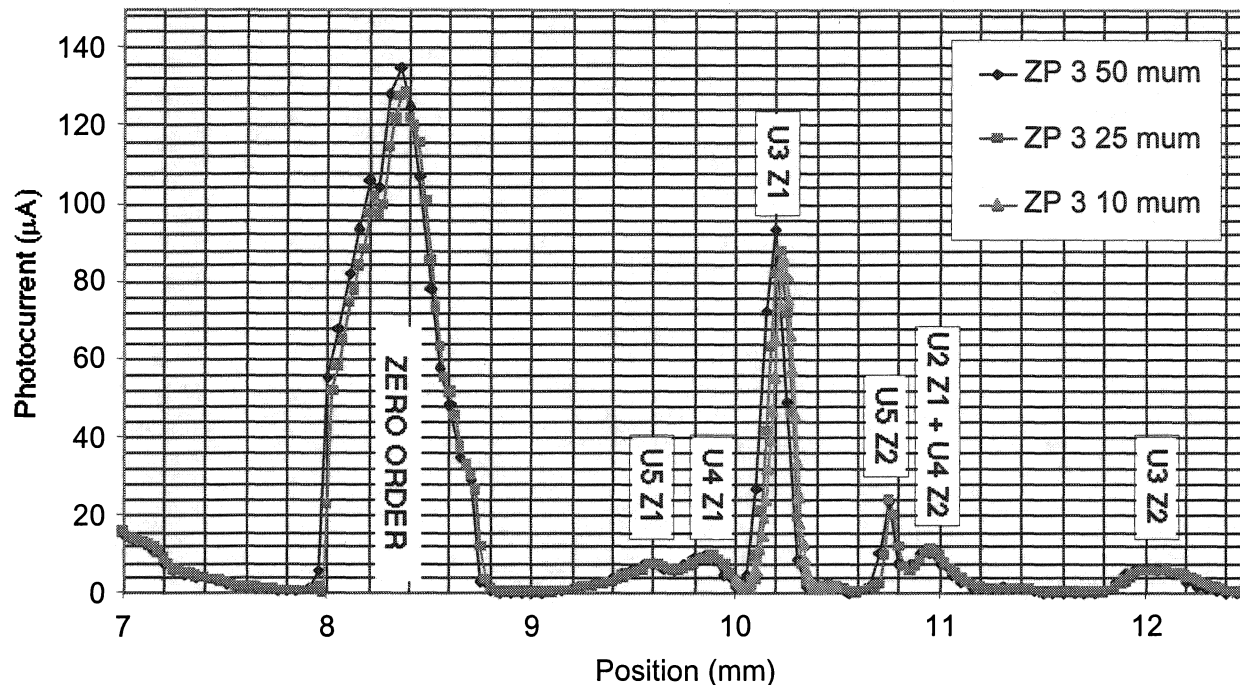


Fig. 9. The monochromator output spectrum.

We do not have a measurement of the actual resolution of the system but we have indirect evidence from the quality of the diffraction patterns that we collect. The monochromator resolution determines the coherence length of the x-ray beam and this impacts the diffraction pattern by destroying the contrast of interference fringes due to rays from the extremities of the sample above the diffraction angle where their path difference exceeds the coherence length. This effect was our reason for building the monochromator. We have not seen any loss of contrast of the speckle at the edges of the pattern and from this we roughly estimate that the resolution is at least 500.

## 9. CONCLUSION

We have reported a successful effort to design and build an off-axis zone-plate monochromator for an ALS undulator beam for diffraction experiments. In particular we have shown how the consequences of the beam power can be calculated and how heat removal pathways can be provided for in the design. We have shown the performance of the beam line and describe its success in producing good diffraction patterns.

## 10. ACKNOWLEDGEMENTS

This work was supported by the Director, Office of Energy Research, Office of Basic Energy Sciences, Materials Sciences Division of the U. S. Department of Energy, under Contract No. DE-AC03-76SF00098

## 11. REFERENCES

1. Butkov, E., *Mathematical Physics*, Addison-Wesley, Reading, 1968.
2. Carslaw, H. S., J. C. Jaeger, *Conduction of Heat in Solids*, Oxford University Press, Oxford, 1959.
3. Graper, E., Lebow Company, 5960 Mandarin Ave, Goleta, CA 93117, USA.
4. Kirz, J., *J. Opt. Soc. Am.*, **64**, 301-309 (1974).
5. Niemann, B., P. Guttman, D. Hambach, G. Schneider, D. Weiss, G. Schmahl, *Nucl. Instrum. Meth.*, **A467-468**, 857-860 (2001).
6. Niemann, B., D. Rudolph, G. Schmahl, *Opt. Comm*, **12**, 160-163 (1974).
7. Timoshenko, S., S. Woionowsky-Krieger, *Theory of Plates and Shells*, McGraw-Hill, New York, 1959.
8. Wood, J., Thermionics Vacuum Products, 231-B Otto St, Port Townsend, WA 98368, USA.